Journal of Ovonic Research Vol. 16, No. 6, November - December 2020, p. 397 - 404

STRUCTURAL AND PHOTOELECTRONIC FEATURES OF NOVEL VANADATE GLASS

H. H. HEGAZY[a,b], I. M. ASHRAF[a,c], H. ALGARNI[a], M. REBEN[d], S. RAFIQUE[e], I. GRELOWSKA[d], E. YOUSEF[a,b,*]

[a]*Physics Dep., Faculty of Science, King Khalid University, P. O. Box 9004, Abha, Saudi Arabia*

[b]*Physics Dep., Faculty of Science, Al- Azhar University, Assiut branch, Assiut, Egypt*

[c]*Physics Dep., Faculty of Science, Aswan University, Aswan, Egypt.*

[d]*Faculty of Materials Science and Ceramics, AGH – University of Science and Technology, al. Mickiewicza 30, 30-059 Cracow, Poland*

[e]*Multidisciplinary Nanotechnology Centre, College of Engineering, Swansea University, Swansea SA1 8EN, United Kingdom*

A recent vanadate glass within the composition as follows; $50V_2O_5$-$30Ag_2O$- 20SrO was prepared in the mol % through a melt-quenching technique. In this paper, the glass transition,T_g, softening temperature, T_s, and the peak of crystallization, T_p, of the present glass determined by using differential thermal analysis (DTA). Moreover, the transient photoconductivity measured at different temperatures in the range 294- 500 K with the intensity of illumination such as; 2000, 3500, 5900, 9400, 13900, 19700, and 26000 lx. The results of dark conductivity σ_d and photoconductivity σ_{ph} obtained that the conduction mechanism in present glass having two regimes activation energy at the temperature range from 294 to 500 K. The value of σ_{ph} and σ_d at 297 K was equal 2.604×10^{-3} $\Omega^{-1}\cdot$ cm^{-1} and 2.604×10^{-3} $\Omega^{-1}\cdot$ cm^{-1}, respectively. Herein the values of activation energy ΔE_{1ph} and ΔE_{2ph} *are* equal to 0.285 and 0.052 eV for region Ith and II, respectively. Both σ_d and σ_{ph} increases linearly with a voltage change in the studied range from 0.2 to 5.0 V. The XRD-pattern shows a distinct line attributed to the crystalline phase $Sr_2V_2O_7$ (ICDD card: 00-048-0145) moreover, the diffraction peaks at 2θ= 38.3^o, 44.5^o, and 64.8^o are assigned to (111), (200) and (220) peaks of Ag (JCPDS4-0783). The crystallite size of the Ag^+ with heat treatment of present glass, which found that equal micro-sized particle ≅7 μm in the glass matrix. Finally, we found that, the σ_{ph} value of the prepared glass is larger than that compared to different glass compositions reported in the literature. Hence the prepared glass is promising as a candidate in optoelectronic devices.

(Received October 3, 2020; Accepted December 8, 2020)

Keywords: Structural, XRD, Scanning electron microscope, Thermal, Photoconductivity, Oxide glass

1. Introduction

Amorphous glasses have recently drawn great attention due to the use of oxygen isolation catalysis in fuel cells and cathode material in solid-state devices [1], Superionic oxide glasses in particular are of great importance because they have high thermal stability [2, 3]. Many authors have attracted the attention [4- 8]studies DC conductivity of semiconducting glasses with composition; AgI- Ag_2O- B_2O_3, AgI- $AgPO_3$, Ag_2O- GeO_2, AgI- Ag_2O- P_2O_5, AgI- Ag_2O- V_2O_5 and AgI- Ag_2O- V_2O_5- P_2O_5. Otherwise a few reports about photoconductivity studies of oxide glasses containing Ag_2O, V_2O_5 are available in the literature. However, Ag^+ doped glasses with a higher content of Ag were also found to be ionic or superionic electrical conductors at room temperature [9].

Also, the structure of, Sr, and other V_2O_5 glasses [10, 11] have been investigated, otherwise, the photoconductivity of these glasses was not reported. Besides, V_2O_5-based glasses have attracted interest as it is possible to use in solid-state devices, IR optical fiber, optical and

*Corresponding authors: omn_yousef2000@yahoo.com

electrical memory switching as a cathode material. The semiconducting nature of vanadate glasses modified with a transition metal, TM, occurs from an unpaired $3d^1$ electron hopping two or more valence states, that is from a V^{4+} site to a V^{5+} site [12, 13]. Because the unpaired electron creates polarization around the, TM, ion, conduction can be characterized as a polaron-based model. We can develop photosensitivity parameters of semiconducting oxide glasses that can use in photoconductor applications at low bias voltage. Moreover, produce and identifying low-cost solar cells, high-photosensitivity, and safety photoconductors.

As mention above, we prepared novel glass with composition; $50V_2O_5$-$30Ag_2O$-20SrO, and calculated dark conductivity σ_d, photoconductivity σ_{ph} at different intensities, activation energy ΔE_{1ph} and ΔE_{2ph}, the photosensitivity parameters are estimated, which can be used as a candidate in optoelectronic devices.

2. Materials and methods

A fast quenching technique (melt quenching) synthesized the glass with the composition mol percent $50V_2O_5$- $30Ag_2O$- 20SrO. Powdered raw silica crucibles have been brought to the air at 950 0C for 30 min in an electric furnace. The high viscosity melt was then cast on a steel mold. The sample was then put in an annealing oven and held at 440 ^{0}C for 2 hours. The furnace was then removed, so the section of the glass could be cooled. Through the differential thermal analysis technology (Shimadzu DTA 50), the glass transition temperature), (temperature relaxation (Ts), the starting crystallization temperature (Tc), and the top crystallization temperature have been measured.

The sample was examined by X-ray diffraction, (Siemens D 6000), scanning electron microscopy (SEM) a JEOL ^{TM} Model JSM-T330 [14]. The material used in electrical measurements was placed in a cryostat (LN Oxford DN1704-type) on the cold finger, which was evacuated to about 10^{-4} Torr. An opaque, non-conducting mask was placed over the sample to illuminate only the aforementioned area. There's a hole in the cryostat 's cold finger where the non-conducting mask was located, as shown in Fig. 1.

A digital temperature controller (Oxford ITC601-type) operated inside the cryostat. Silver paste was used to create contacts between samples and metal electrodes. The linear variations of the I–V function in the entire investigated voltage confirmed the Ohmic behavior of the contacts.

A 1000 W tungsten lamp, which was attached to a variac to change the light intensity at the sample surface, induced excitation. The modification was conducted for the longest distance between the source of light and the sample from which to achieve reasonably accurate spectral distribution. Using an optical device composed of two convex lenses, the light was focussed on the sample to allow a homogeneous illumination of the area between the two electrodes. The proper safety was taken to minimize the thermal influence of the light source, where the instrument was placed within the evacuated cryostat on the cold finger (10^{-4} Torr). Additionally, by sending the light beam via a water filter, heat emission from the light source was avoided. The measurement setup is fitted with a simple air-cooling ventilator. To calculate the PC's reliance on the light strength, a programmable digital electrometer (6517B Keithley Instrument) was used to test the voltage added to the light source. The net photocurrent was calculated by subtracting the dark current from the photocurrent measured. After reaching a steady-state value, the total current (in the presence of light) was recorded at each point. After such an illumination change this value is often obtained 30 s later. A Carl Zeiss M4GII-type monochromator was used for the measurement of the dc-PC.

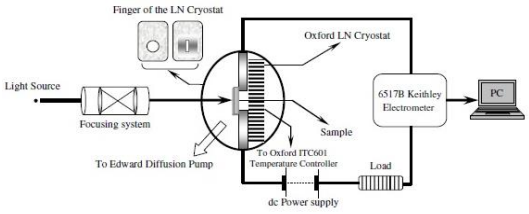

Fig. 1. Schematic diagram of the experimental arrangements used in the photoconductivity measurements.

3. Results and discussion

The sample's amorphous nature was verified using X-ray diffraction (XRD) was shown in Fig. 2A. It shows a broad scattering at low angles suggesting and there was no identification of sharp peaks in the X-ray diffraction patterns which indicated that the sample was amorphous after prepared. Fig. 2b shows a prepared glass DTA profile. A characteristic temperature such as glass transition temperature, T_g=464 ^{0}C, softening temperature, T_s=527 ^{0}C, crystallization process starting temperature T_c=553 ^{0}C and crystallization peak, T_p=560 ^{0}C is obtained from this profile. Herein the prepared glasses give a high thermal stability value, (T_c-T_g), which is equal, 89 ^{0}C.

Fig. (3a, b) shows the photoconductivity (σ_{ph}) and dark conductivity (σ_d) of the prepared glasses for different temperatures, respectively. The dark conductivity (σ_d) can be expressed by the Arrhenius equation as following [15];

$$\sigma_d = \sigma_0 \exp\left(\frac{-\Delta E}{kT}\right) \quad (1)$$

where ΔE is the activation energy of the dc conduction and k is the Boltzmann's constant. It is shown that the electrical conductivity rises with the increasing temperature. Both ΔE and σ_d values are calculated from the slope of the curve in Fig. (3a, b). In the studied glass, the curve can be fitted by two approximately linear regions (see region I and II in Fig. 3a). This means that in two different temperature ranges, also two different values of activation energy ΔE_{1ph} and ΔE_{2ph} are observed. The activation energy corresponds to the depth of the traps in the gap. The values of ΔE_{ph} *are* equal to 0.285 and 0.052eV for region Ith and II, respectively. The σ_{ph} value at 297 K equals 2.604 × 10^{-3} $\Omega^{-1}\cdot$ cm^{-1}. In Fig. (3b), a plot of ln (σ_d) is shown as a function of the reciprocal temperature. Also here, the curve can be approximated by two straight lines for two different temperature ranges. The attributed activation energies for the region I and II are 0.228 and 0.143 eV, respectively. The σ_d value at 297 K is 1.726×10^{-3} $\Omega^{-1}\cdot$cm^{-1}.

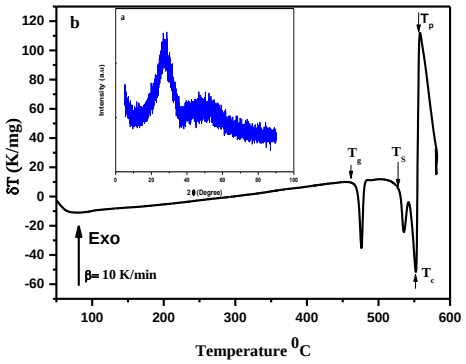

Fig. 2. (a, b) XRD-pattern of the prepared glass with the composition 50$V_2O_5\cdot$30$Ag_2O\cdot$20SrO in mol%. Fig. 2b: DTA-profile of the prepared glass 50$V_2O_5\cdot$30$Ag_2O\cdot$20SrO at a heating rate 15K/min.

The plot σ_{ph} vs 1/KT and σ_d vs 1/KT are shown in Fig. (3c) and can be described as follows:

(i) At a high temperature above 392 K, the photocurrent is smaller than the dark current, $\sigma_d > \sigma_{ph}$. Then the concentration of thermal carriers exceeds that of photocarriers.

(ii) At the temperature T= 392 K, the photocurrent equal the dark current, $\sigma_d \cong \sigma_{ph}$.

(iii) At low temperature (T< 392 K), the photocurrent is much larger than the dark current, $\sigma_d < \sigma_{ph}$. where increasing the recombination rate of carries and decreasing of Ag^+ ions.

The photosensitivity value $\left(\frac{\sigma_{ph}}{\sigma_d}\right)$ is an important parameter in photoconductivity measurements; it limits the possible use of the material in photoconductive devices. In the present glasses the value of $\left(\frac{\sigma_{ph}}{\sigma_d}\right)$ is equal to 1.51. Hence, in this case σ_d is smaller than σ_{ph} due to the increased formation of photogenerated carriers in the prepared glasses matrix. In the literature, values of σ_{ph} are reported for different glasses systems. In glasses system with composition Se-Te-Pb the σ_{ph} values are in the range from 8.6×10^{-8} to 1.11×10^{-4} $\Omega^{-1}\cdot cm^{-1}$ and σ_d values in the range 1.25×10^{-9} to 5.56×10^{-4} $\Omega^{-1}\cdot cm^{-1}$ [15]. In the studied glasses system, Se-Ge-Ag, σ_{ph} -values are between 5.32×10^{-9} to 6.07×10^{-8} $\Omega^{-1}\cdot cm^{-1}$ and σ_d values in the range 1.39×10^{-9} to 7.89×10^{-8} $\Omega^{-1}\cdot cm^{-1}$ [16]. The σ_{ph} and $\sigma_d$values of around 1.97×10^{-7} and 2×10^{-8} $\Omega^{-1}\cdot cm^{-1}$ were reported for Ge-Se-Sn glasses [17]. For Se-In-Sb glasses [18] the σ_{ph} -values between 1.0×10^{-8} and 5.00×10^{-8} $\Omega^{-1}\cdot cm^{-1}$ were reported; the $\sigma_d$values were around 1.67×10^{-9} $\Omega^{-1}\cdot cm^{-1}$. In the glass system Se-Te-Ge the σ_{ph} values were in the range from 4.57×10^{-8} to 3.57×10^{-7} $\Omega^{-1}\cdot cm^{-1}$ and the σ_d values in the range 4.29×10^{-9} to 2.46×10^{-6} $\Omega^{-1}\cdot cm^{-1}$ [19]. In comparison to previous data reported in the literature [15-19], the σ_{ph} value of prepared glasses $50V_2O_5\cdot$ $30Ag_2O\cdot$ 20SrO are 10 to 10^6 times larger than other glass systems. Hence that this glass may be promising can be used in photoelectronic devices.

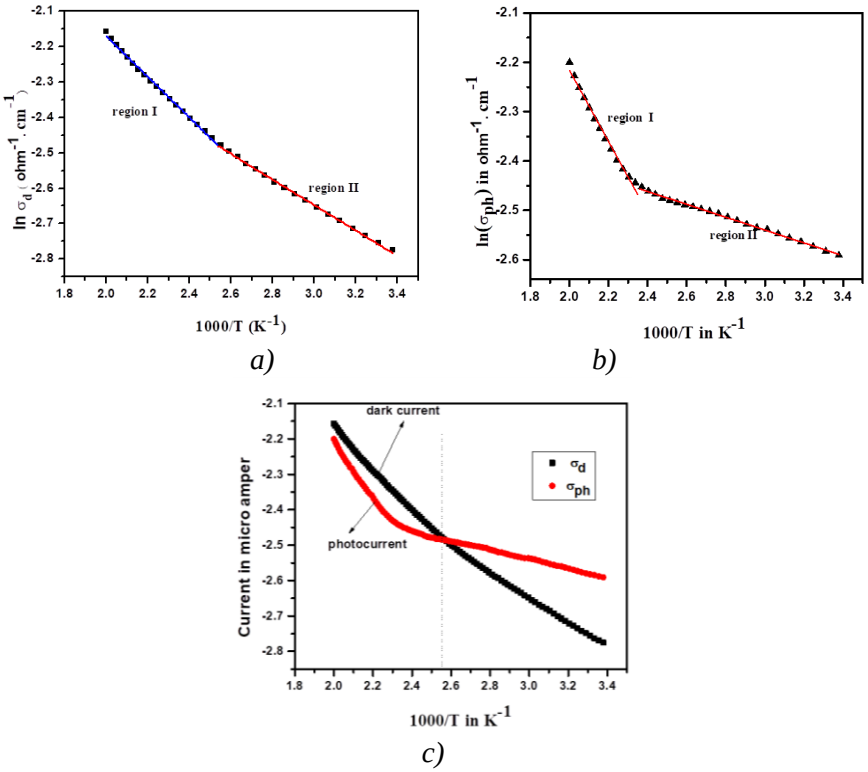

Fig. 3. (a) Temperature dependencies of the photoconductivity, σ_{ph}, of prepared glass; (b) Temperature dependencies of dark conductivity, σ_d. of prepared glass;(c) Temperature dependencies of photoconductivity, σ_p and dark conductivity, σ_d.

This means that the migration and aggregation of silver atoms in the prepared glasses are being sensitive to both the light intensity and the temperature. Moreover, it can also be seen from Figs. 4 that the photocurrent increases with the light intensity in the range from 2000 to 26000 lx. The same behavior has already been reported in $TlInSe_2$ single crystals [20]. The photoconduction mechanism in amorphous materials is based on the recombination kinetics using the charged defect model [20- 22]. The bonding defects may exist in three charging states, denoted as D^+, D^- and D^0, where D is referred to the dangling bond defect, and the superscripts represent the charging states. Once the photo-induced formation of D^0 centers from bonding state (NB) at low energy of the photo-excited state and attributed to improved photo-conductivity. Otherwise, the D^0 centers are called quasi-stable leads to the decrease in photocurrent due to the formation of D^- and D^+ centers from D^0 centers with the increasing the exposure time at room temperature. The D^- centers can be formed from D^0 centers and thermal energy at room temperature through the reaction $D^0 - h \leftrightarrow D^-$, where h denotes a "hole," D^- centers will represent as trapping or recombination centers. Therefore the decrease in photocurrent may have occurred, which decrease in carrier existence due to increased recombination in the prepared glasses V_2O_5- Ag_2O- SrO.

Fig. 4 shows the dependency of the dark and the photocurrent of the present glasses on the applied voltage. The figure indicates that both dark current and photocurrent increases linearly with a voltage change in the studied range from 0.2 to 5.0V. These experimental results reveal that the present glass has a strong microampere present at low voltages and therefore improves the lighting leading to the production of free carriers. The studied glasses obtained that high sensitivity to light in comparison to the other glasses such as Se-Te-Pb, Se-Ge-Ag, Se-Te-Ge, and Ge-Se-Sn [17, 20- 24]. The ln (σ_{ph}) vs. ln F plots at different temperatures were seen in Fig. 5. It shows that the σ_{ph} photoconductivity meets a power law of intensity (F) i.e $\sigma_{ph} = constant \cdot F^{\gamma}$, with $0.57 \leq \gamma \geq 0.59$. This value that varies between 0.5 and 1.0 means that the mobility gap of the glassy matrix is permanent and the resultant recombination mechanism is bimolecular, under which the recombination value of the electrons is commensurate with the numbers of holes. We note that in a single tarp analysis for the case $\gamma = 0.5$ this corresponds to the case of bimolecular recombination, while $\gamma = 1.0$ is attributed to monomolecular recombination.

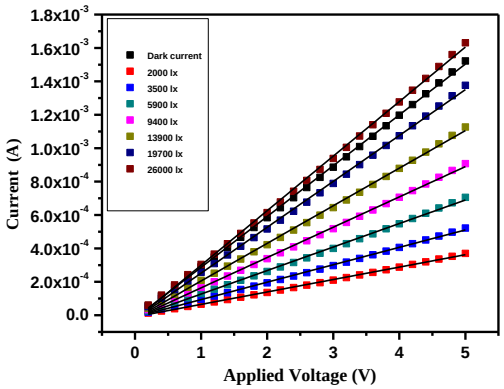

Fig. 4. The dark and photocurrents of prepared glass, with an applied voltage at different intensities.

Fig. 6 obtain the increase and decay of the photocurrent at different illumination from 2000 to 26000 Lux. Photocurrent measurements were performed by exposing the studied sample to light, and the photocurrent registered at the same time until the current became saturated. Then the light was turned off and the photocurrent decay was reported with time. The resulting decay of the photocurrent is fast in the beginning and then becomes slower. This behavior has already been observed in glasses Ge- Se- Sn [17]. Fig. 6 indicates that the presence of photocurrent increases monotonously and tends to a constant value. The phase of decay can be clarified through the concept of a lifetime, τ_d, of variation [20].

$$\tau_d = -\left[\frac{1}{I_{ph}}\frac{d(I_{ph})}{dt}\right]^{-1} \quad (2)$$

The average photocurrent at t = 0 is from the slope of I_{ph} and time (i.e. I_{ph} is the max. value at t = 0). According to this definition, the differential lifetime, $\tau_{d,}$ of the carrier, increases otherwise in the case of a (mono)exponential decay, the lifetime of the carrier exceeds throughout the time interval observed. Using Fig. 7 and the above equation (2), the differential lifetime values were determined by finding the slopes at various values of the time of decay, and for all the light intensities examined. Such values were used in different phases of illumination to achieve the time dependency of the differential lifetime. A similar analysis for other glass systems has already been reported in glasses Se-Ge-Ag, Se-Te-Ge, and Ge-Se-Sn.

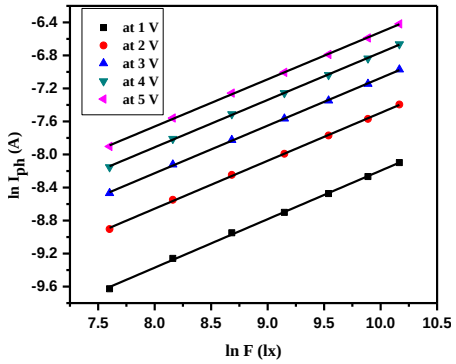

Fig. 5. ln σ_{ph} with ln F, of prepared glass at a different voltage.

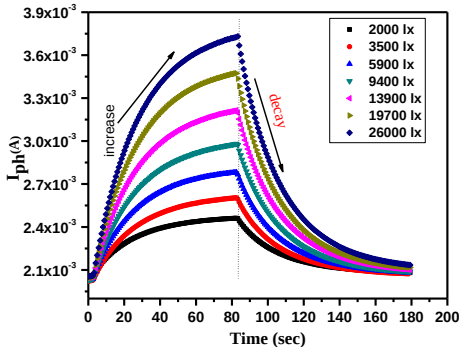

Fig. 6. Increase and decay of photocurrent (σ_{ph}) at different intensities.

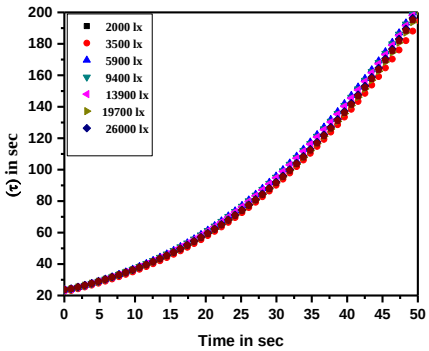

Fig. 7. Time dependencies of the differential lifetime for prepared glass at different intensities.

Fig. 8 demonstrates patterns of glass X-ray powder diffraction with composition $50V_2O_5$-$30Ag_2O$- 20SrO in mol level, tempered for 2 h at 550 ^oC. The XRD-pattern shows a distinct line and hence is crystallized. In the thermally annealed glass, peaks attributed to the crystalline phase $Sr_2V_2O_7$ (ICDD card: 00-048-0145) are detected. Additionally, lines attributable to Ag with no sharp and weak diffraction peaks were observed. The diffraction peaks at 38.3, 44.5, and 64.8 are assigned to (111), (200) and (220) peaks of Ag (JCPDS4-0783). Tsuzuku et al. [25] studied the effect of Ag addition on the crystallization of CaO-SrO-BaO-Al_2O_3-SiO_2-TiO_2 glasses. They concluded Ag ions were dissolved in the glass phase and the Ag ion acts as a nucleation agent so that crystallization was promoted. This might also have occurred in prepared glass. Figure (9) shows an SEM micrograph from the cross-section of a glasses tempered at 550 ^oC for 2 h. In this microstructure graph, spherical silver particles were precipitated in the glass matrix which should lead to increasing the value of photocurrent of prepared glasses. The crystallite size of the Ag^+ with heat treatment, which found that equal ≅7 μm in the glass-ceramic matrix (see Fig. 9).

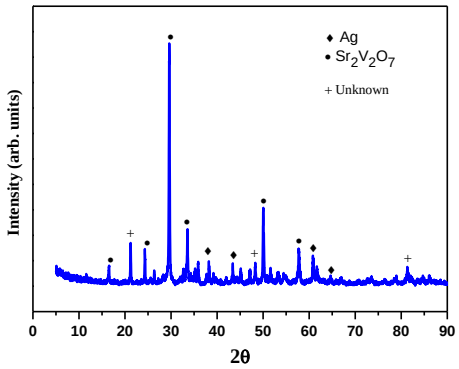

Fig. 8. X- ray diffraction patterns of the prepared glass tempered at 550 ^oC for 2 h.; where (● Ag, ♦ $Sr_2V_2O_7$, + Unknown.

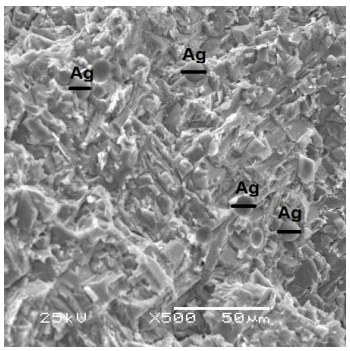

Fig. 9. SEM micrograph of prepared glass tempered at 550 ^oC for 2 h.

4. Conclusion

Dark and photoconductivity measurements were performed in $50V_2O_5$- $30Ag_2O$- 20SrO glass. The photoconductivity of the prepared glasses is strongly dependent on the temperature at various intensities suggested that the photoconductivity is activated thermally. At low temperature, the photocurrent increase with increasing the recombination rate of carries. Moreover, the transient decay in photocurrent measurements depends on the intensity of the light used for illumination. The photocurrent initially decays very fast and later slows down. The photosensitivity parameters (σ_{ph}/σ_d) value of present glasses equal 1.51 hence can be used in the future as candidates for optoelectronic switching devices. The spherical particles of Ag in the glass-ceramic matrix tempered at temperatures 550 ^oC for 2h were created.

Acknowledgments

The authors extend their appreciation to the Deanship of Scientific Research Khalid University (KKU) for funding this research project number (R.G. P2/63/40).

References

[1] C. A. Angell, Annu. Rev. Phys. Chem. **43**, 693 (1992)
[2] T. Minami, J. Non-Cryst. Solids **56**, 15 (1983)
[3] A. Ghosh, D. Dutta, S. Kabi, A. Ghosh, J. Appl. Phys. **105** (2009) 064107
[4] H. Takahashi, Y. Hiki, T. Sakuma, Y. Morii, **90**, (1251996).
[5] Z. Wisniewski, R. Wisniewski, J. L. Nowinski, Solid State Ionics **157**, 275 (2003).
[6] Y. Kowada, H. Adachi, M. Tatsumisago, T. Minami, **234**, 497 (1998).
[7] H. Takahashi, K. Shishitsuka, T. Sakuma, Y. Shimojo, Y. Ishii, Solid State Ionic **115**, 685 (1998).
[8] R. Maminska, M. Kucharek, P. Jozwiak, J. Garbarczyk, A. Dybko, Wroblewski, Microchim. Acta **159**, 311 (2007).
[9] J. L. Pascual, L. Seijo, Z. Barandiaran, J. Chem. Phys. **98**(12), 9715 (1993).
[10] S. Sen, A Ghosh, J. Mater. Res. **15**, 995 (2000).
[11] S. Sindhu, S. Sanghi, A. Agrawal, Sonam, V. P. Seth, N. Kishore, Physica B **365**, 65 (2005).
[12] G. S. Linsley, A. E. Owen, F. M. Hayatee, J. Non-Cryst. Solids **4**, 208 (1970).
[13] G. D. Khattak, A. Mekki, J. Non-Cryst. Solids **70**, 1330 (2009).
[14] I. M. Ashraf, M. Farouk, F. Ahmed, M. M. Elokr, M. M. Abdel Aziz, E. S. Yousef, Chalcogenide Letters **16**(7), 327 (2019).
[15] N. Kushwaha, V. S. Kushwaha, R. K. Shukla, A. Kumar, J. Non. Cryst. Solids **351**, 3414 (2005).
[16] R. S. Sharma, S. Singh, D. Kummar, A. Kumar, Physics B **369**, 227 (2005).
[17] A. Thakur, V. Sharma, P. S. Chandel, N. Goyal, G. S. S. Sani, S. K. Tripathi, J. Mater Sci. **41**, 2327 (2006).
[18] S. Shukla, S. Kumar, Chalcogenide Letters **6**, 695 (2009).
[19] D. Kumar, S. Kumar, Turk J. Phys. **29**, 91 (2005).
[20] A. M. Badr, I. M. Ashraf, Phys. Scr. 03570**486**, (2012).
[21] Mohd. Shkir, Mohd. Taukeer Khan, I. M. Ashraf, S. AlFaify, Ahmed Mohamed El-Toni, Ali Aldalbahi, Hamid Ghaithan, AslamKhan, Ceramics International A. **45**(17), 21975 (2019).
[22] Mohd. Shkir, I. M. Ashraf, Kamlesh V. Chandekar, I. S. Yahia, Aslam Khan, H. Algarni, S. AlFaify, Sensors and Actuators A **301**, 111749 (2020).
[23] Mohd. Shkir, I. S. Yahia, V. Ganesh, Y. Bitla, I. M. Ashraf, Ajeet Kaushik, S. AlFaify, Scientific Reports **8**, 13806 (2018).
[24] M. Kamboj, F. Mohammadi, Thin Solid Films **518**, 1585 (2009).
[25] K. Tsuzuku, H. Kishi, Proc. VII European Society of Glass Science and Technology Conf., Athens, Greece, 25- 28 April 2004, Glass Technol., 46 (2005) 134.